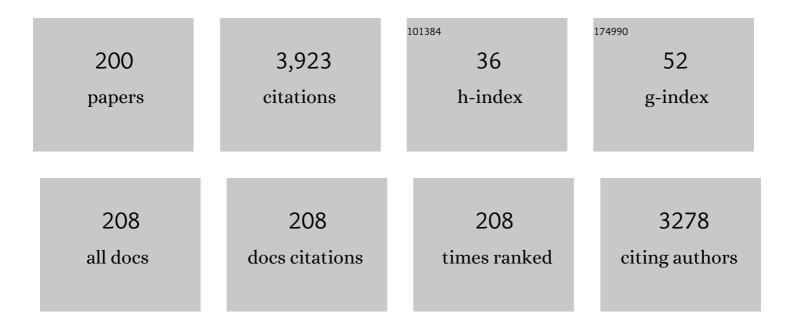
Koji Fushimi

List of Publications by Year in descending order

Source: https://exaly.com/author-pdf/6675949/publications.pdf Version: 2024-02-01



#	Article	IF	CITATIONS
1	Chameleon Luminophore for Sensing Temperatures: Control of Metalâ€toâ€Metal and Energy Back Transfer in Lanthanide Coordination Polymers. Angewandte Chemie - International Edition, 2013, 52, 6413-6416.	7.2	313
2	Fast migration of fluoride ions in growing anodic titanium oxide. Electrochemistry Communications, 2007, 9, 1222-1227.	2.3	160
3	An agar-based silver silver chloride reference electrode for use in micro-electrochemistry. Electrochemistry Communications, 1999, 1, 180-183.	2.3	152
4	Corrosion behaviour of ferrite and austenite phases on super duplex stainless steel in a modified green-death solution. Corrosion Science, 2014, 89, 111-117.	3.0	88
5	An SECM observation of dissolution distribution of ferrous or ferric ion from a polycrystalline iron electrode. Electrochimica Acta, 2001, 47, 121-127.	2.6	77
6	High capacitance B/C/N composites for capacitor electrodes synthesized by a simple method. Journal of Power Sources, 2010, 195, 1739-1746.	4.0	66
7	Heterogeneous Growth of Anodic Oxide Film on a Polycrystalline Titanium Electrode Observed with a Scanning Electrochemical Microscope. Journal of the Electrochemical Society, 2000, 147, 524.	1.3	61
8	Electropolishing of NiTi shape memory alloys in methanolic H2SO4. Electrochimica Acta, 2006, 52, 1290-1295.	2.6	61
9	Sevenâ€Coordinate Luminophores: Brilliant Luminescence of Lanthanide Complexes with <i>C</i> _{3<i>v</i>} Geometrical Structures. European Journal of Inorganic Chemistry, 2015, 2015, 4769-4774.	1.0	60
10	Spark anodizing of β-Ti alloy for wear-resistant coating. Surface and Coatings Technology, 2007, 201, 8730-8737.	2.2	59
11	Thermostable Organoâ€phosphor: Lowâ€Vibrational Coordination Polymers That Exhibit Different Intermolecular Interactions. ChemPlusChem, 2012, 77, 277-280.	1.3	58
12	Anodic dissolution of titanium in chloride-containing ethylene glycol solution. Electrochimica Acta, 2009, 55, 258-264.	2.6	55
13	Triboluminescence of Lanthanide Coordination Polymers with Faceâ€ŧoâ€Face Arranged Substituents. Angewandte Chemie - International Edition, 2017, 56, 7171-7175.	7.2	54
14	Enhanced Luminescence of Asymmetrical Seven oordinate Eu ^{III} Complexes Including LMCT Perturbation. European Journal of Inorganic Chemistry, 2017, 2017, 3843-3848.	1.0	53
15	Anodic dissolution of titanium in NaCl-containing ethylene glycol. Electrochimica Acta, 2008, 53, 3371-3376.	2.6	50
16	Use of a Liquid-Phase Ion Gun for Local Breakdown of the Passive Film on Iron. Journal of the Electrochemical Society, 2000, 147, 552.	1.3	48
17	Current distribution during galvanic corrosion of carbon steel welded with type-309 stainless steel in NaCl solution. Corrosion Science, 2008, 50, 903-911.	3.0	47
18	Spiral Eu(<scp>iii</scp>) coordination polymers with circularly polarized luminescence. Chemical Communications, 2018, 54, 10695-10697.	2.2	47

Којі Ғизнімі

#	Article	IF	CITATIONS
19	Corrosion protection of epoxy coating with pH sensitive microcapsules encapsulating cerium nitrate. Corrosion Science, 2019, 148, 188-197.	3.0	47
20	Depassivation–repassivation behavior of type-312L stainless steel in NaCl solution investigated by the micro-indentation. Corrosion Science, 2009, 51, 1545-1553.	3.0	46
21	Luminescent Europium(III) Coordination Zippers Linked with Thiopheneâ€Based Bridges. Angewandte Chemie - International Edition, 2016, 55, 12059-12062.	7.2	46
22	Chiral lanthanide lumino-glass for a circularly polarized light security device. Communications Chemistry, 2020, 3, .	2.0	45
23	Preparation of self-organized porous anodic niobium oxide microcones and their surface wettability. Acta Materialia, 2009, 57, 3941-3946.	3.8	43
24	Anisotropic corrosion of iron in pH 1 sulphuric acid. Electrochimica Acta, 2010, 55, 7322-7327.	2.6	43
25	Importance of water content in formation of porous anodic niobium oxide films in hot phosphate–glycerol electrolyte. Electrochimica Acta, 2009, 54, 946-951.	2.6	42
26	Effect of Ligand Polarization on Asymmetric Structural Formation for Strongly Luminescent Lanthanide Complexes. European Journal of Inorganic Chemistry, 2013, 2013, 5911-5918.	1.0	42
27	Chameleon Luminophore for Sensing Temperatures: Control of Metalâ€toâ€Metal and Energy Back Transfer in Lanthanide Coordination Polymers. Angewandte Chemie, 2013, 125, 6541-6544.	1.6	42
28	Luminescent Coordination Glass: Remarkable Morphological Strategy for Assembled Eu(III) Complexes. Inorganic Chemistry, 2015, 54, 4364-4370.	1.9	42
29	Effect of Hydrogen Sulfide Ions on the Passive Behavior of Type 316L Stainless Steel. Journal of the Electrochemical Society, 2015, 162, C685-C692.	1.3	41
30	Cross-section corrosion-potential profiles of aluminum-alloy brazing sheets observed by the flowing electrolyte scanning-droplet-cell technique. Electrochimica Acta, 2008, 53, 2529-2537.	2.6	40
31	Spark anodizing behaviour of titanium and its alloys in alkaline aluminate electrolyte. Corrosion Science, 2009, 51, 1534-1539.	3.0	40
32	Microelectrode techniques for corrosion research of iron. Electrochimica Acta, 2013, 113, 741-747.	2.6	39
33	Evaluation of Heterogeneity in Thickness of Passive Films on Pure Iron by Scanning Electrochemical Microscopy. ISIJ International, 1999, 39, 346-351.	0.6	38
34	Heterogeneous hydrogen evolution on corroding Fe–3at.% Si surface observed by scanning electrochemical microscopy. Electrochimica Acta, 2007, 52, 4246-4253.	2.6	38
35	Eu(III) Chiral Coordination Polymer with a Structural Transformation System. Inorganic Chemistry, 2017, 56, 5741-5747.	1.9	38
36	A Luminescent Dinuclear Eu ^{III} /Tb ^{III} Complex with LMCT Band as a Singleâ€Molecular Thermosensor. Chemistry - A European Journal, 2018, 24, 1956-1961.	1.7	38

#	Article	IF	CITATIONS
37	Thermo-sensitive luminescent materials composed of Tb(III) and Eu(III) complexes. Materials Letters, 2014, 130, 91-93.	1.3	37
38	Critical Role of Energy Transfer Between Terbium Ions for Suppression of Back Energy Transfer in Nonanuclear Terbium Clusters. Scientific Reports, 2016, 6, 37008.	1.6	37
39	Initiation of a Local Breakdown of Passive Film on Iron due to Chloride Ions Generated by a Liquid-Phase Ion Gun. Journal of the Electrochemical Society, 2001, 148, B450.	1.3	36
40	Influence of Substrate Dislocation on Passivation of Pure Iron in pH 8.4 Borate Buffer Solution. Journal of the Electrochemical Society, 2010, 157, C231.	1.3	33
41	Ligandâ€Assisted Back Energy Transfer in Luminescent Tb ^{III} Complexes for Thermosensing Properties. Chemistry - A European Journal, 2018, 24, 17719-17726.	1.7	33
42	Grain-Dependent Passivation of Iron in Sulfuric Acid Solution. Journal of the Electrochemical Society, 2014, 161, C594-C600.	1.3	32
43	Longâ€Range LMCT Coupling in Eu ^{III} Coordination Polymers for an Effective Molecular Luminescent Thermometer**. Chemistry - A European Journal, 2021, 27, 264-269.	1.7	31
44	Depth profile analysis of thin passive films on stainless steel by glow discharge optical emission spectroscopy. Corrosion Science, 2009, 51, 1554-1559.	3.0	30
45	A highly luminescent Eu(iii) complex based on an electronically isolated aromatic ring system with ultralong lifetime. Dalton Transactions, 2018, 47, 7327-7332.	1.6	30
46	Influence of silicon on the growth of barrier-type anodic films on titanium. Electrochimica Acta, 2007, 52, 6834-6840.	2.6	29
47	Passivation Behavior of Type-316L Stainless Steel in the Presence of Hydrogen Sulfide Ions Generated from a Local Anion Generating System. Electrochimica Acta, 2016, 220, 304-311.	2.6	29
48	Microelectrochemistry of dual-phase steel corroding in 0.1 M sulfuric acid. Electrochimica Acta, 2013, 114, 83-87.	2.6	28
49	Enhancement of Optical Faraday Effect of Nonanuclear Tb(III) Complexes. Inorganic Chemistry, 2014, 53, 7635-7641.	1.9	26
50	Enhanced Light Storage of SrAl ₂ O ₄ Glassâ€Ceramics Controlled by Selective Europium Reduction. Journal of the American Ceramic Society, 2015, 98, 423-429.	1.9	26
51	Effective Photo―and Triboluminescent Europium(III) Coordination Polymers with Rigid Triangular Spacer Ligands. Chemistry - A European Journal, 2017, 23, 2666-2672.	1.7	26
52	In situ X-ray absorption spectroscopy for identification of lead species adsorbed on a nickel surface in acidic perchlorate solution. Journal of Electroanalytical Chemistry, 2012, 671, 7-15.	1.9	25
53	Hyper-stable organo-EulII luminophore under high temperature for photo-industrial application. Scientific Reports, 2016, 6, 24458.	1.6	25
54	Effective Photosensitized Energy Transfer of Nonanuclear Terbium Clusters Using Methyl Salicylate Derivatives. Journal of Physical Chemistry A, 2015, 119, 1943-1947.	1.1	24

#	Article	IF	CITATIONS
55	The Role of π–f Orbital Interactions in Eu(III) Complexes for an Effective Molecular Luminescent Thermometer. Inorganic Chemistry, 2020, 59, 5865-5871.	1.9	24
56	Study on initiation of localised corrosion on copper thin film electrode by combinational use of an EQCM with a liquid-phase ion gun. Corrosion Science, 2003, 45, 2657-2670.	3.0	23
57	Development of a novel microstructure fabrication method with co-axial dual capillary solution flow type droplet cells and electrochemical deposition. Electrochimica Acta, 2008, 54, 616-622.	2.6	22
58	Effective Optical Faraday Rotations of Semiconductor EuS Nanocrystals with Paramagnetic Transition-Metal Ions. Journal of the American Chemical Society, 2013, 135, 2659-2666.	6.6	22
59	Structural Manipulation of Triboluminescent Lanthanide Coordination Polymers by Side-Group Alteration. Inorganic Chemistry, 2018, 57, 14653-14659.	1.9	22
60	Electronic chirality inversion of lanthanide complex induced by achiral molecules. Scientific Reports, 2018, 8, 16395.	1.6	22
61	Electronic strain effect on Eu(<scp>iii</scp>) complexes for enhanced circularly polarized luminescence. Dalton Transactions, 2020, 49, 5352-5361.	1.6	22
62	Hydrogen generation from a single crystal magnetite coupled galvanically with a carbon steel in sulfate solution. Corrosion Science, 2002, 44, 611-623.	3.0	21
63	Formation of porous anodic films on Ti–Si alloys in hot phosphate-glycerol electrolyte. Electrochimica Acta, 2007, 53, 1775-1781.	2.6	21
64	Solvent-dependent luminescence of eight-coordinated Eu(III) complexes with bidentate phosphine oxide. Journal of Photochemistry and Photobiology A: Chemistry, 2012, 235, 35-39.	2.0	21
65	Enhanced Electric Dipole Transition in Lanthanide Complex with Organometallic Ruthenocene Units. Journal of Physical Chemistry A, 2015, 119, 4825-4833.	1.1	21
66	Passivity of Dual-Phase Carbon Steel with Ferrite and Martensite Phases in pH 8.4 Boric Acid-Borate Buffer Solution. Journal of the Electrochemical Society, 2015, 162, C322-C326.	1.3	21
67	Luminescent Eu(III) coordination polymer cross-linked with Zn(II) complexes. Materials Letters, 2016, 167, 183-187.	1.3	21
68	Coordination Geometrical Effect on Ligand-to-Metal Charge Transfer-Dependent Energy Transfer Processes of Luminescent Eu(III) Complexes. Journal of Physical Chemistry A, 2021, 125, 209-217.	1.1	21
69	Application of the multichannel electrode method to monitoring of corrosion of steel in an artificial crevice. Corrosion Science, 2010, 52, 1179-1186.	3.0	20
70	First Synthesis of EuS Nanoparticle Thin Film with a Wide Energy Gap and Giant Magneto-Optical Efficiency on a Glass Electrode. Journal of Physical Chemistry C, 2012, 116, 19590-19596.	1.5	20
71	Growth and Degradation of an Anodic Oxide Film on Titanium in Sulphuric Acid Observed by Ellipso-microscopy. Electrochimica Acta, 2014, 144, 56-63.	2.6	20
72	Nearâ€IR Luminescent Yb III Coordination Polymers Composed of Pyrene Derivatives for Thermostable Oxygen Sensors. Chemistry - A European Journal, 2019, 25, 12308-12315.	1.7	20

#	Article	IF	CITATIONS
73	A Scanning Electrochemical Microscopic Observation of Heterogeneous Oxygen Evolution on a Polycrystalline Titanium during Anodic Oxidation. Electrochemistry, 2000, 68, 950-954.	0.6	20
74	Stacked nanocarbon photosensitizer for efficient blue light excited Eu(III) emission. Communications Chemistry, 2020, 3, .	2.0	19
75	Trial for Evaluation of Heterogeneity of Passive Film on Iron by a Scanning Electrochemical Microscope. Zairyo To Kankyo/ Corrosion Engineering, 1997, 46, 797-803.	0.0	17
76	Red Luminescent Eu(III) Coordination Bricks Excited on Blue LED Chip. Inorganic Chemistry, 2018, 57, 7097-7103.	1.9	17
77	Effect of underpotential deposition of lead on polarization behavior of nickel in acidic perchlorate solutions at room temperature. Corrosion Science, 2008, 50, 3139-3146.	3.0	16
78	Molecular Design Guidelines for Large Magnetic Circular Dichroism Intensities in Lanthanide Complexes. ChemPhysChem, 2016, 17, 845-849.	1.0	16
79	Photosensitized Luminescence of Highly Thermostable Mononuclear Eu(III) Complexes with π-Expanded β-Diketonate Ligands. Bulletin of the Chemical Society of Japan, 2017, 90, 1287-1292.	2.0	16
80	Triboluminescence of Lanthanide Coordination Polymers with Faceâ€ŧoâ€Face Arranged Substituents. Angewandte Chemie, 2017, 129, 7277-7281.	1.6	15
81	Fabrication of Cu Micro-rods with Co-axial Dual Capillary Solution Flow Type Droplet Cell and Electrodeposition with the Cell. Electrochemistry, 2010, 78, 118-121.	0.6	14
82	Enhanced Magnetoâ€optical Properties of Semiconductor EuS Nanocrystals Assisted by Surface Plasmon Resonance of Gold Nanoparticles. Chemistry - A European Journal, 2013, 19, 14438-14445.	1.7	14
83	Luminescent Thin Films Composed of Nanosized Europium Coordination Polymers on Glass Electrodes. ChemPlusChem, 2016, 81, 187-193.	1.3	14
84	Current transients of passive iron observed during micro-indentation in pH 8.4 borate buffer solution. Electrochimica Acta, 2006, 51, 1255-1263.	2.6	13
85	Reactivity imaging of a passive ferritic FeAlCr steel. Journal of Applied Electrochemistry, 2008, 38, 1339-1345.	1.5	12
86	Novel opto-magnetic silicate glass with semiconductor EuS nanocrystals. Journal of Alloys and Compounds, 2013, 562, 123-127.	2.8	12
87	Effective Europium Coordination Luminophores Linked with Bi- and Tridentate Carbazole Phosphine Oxides for Organic Electroluminescent Devices. Journal of Physical Chemistry C, 2018, 122, 9599-9605.	1.5	12
88	Thermal degradation of anodic niobia on niobium and oxygen-containing niobium. Thin Solid Films, 2008, 516, 991-998.	0.8	11
89	Depassivation–repassivation behavior of a pure iron surface investigated by micro-indentation. Electrochimica Acta, 2010, 55, 1232-1238.	2.6	11
90	Thermostable Eu(III)-nanorod luminophores with effective photosensitized energy transfer. Journal of Alloys and Compounds, 2015, 648, 651-657.	2.8	11

#	Article	IF	CITATIONS
91	Hydrogen Permeation into a Carbon Steel Sheet Observed by a Micro-capillary Combined with a Devanathan-Stachurski Cell. ISIJ International, 2016, 56, 431-435.	0.6	11
92	The relationship between magneto-optical properties and molecular chirality. NPG Asia Materials, 2016, 8, e251-e251.	3.8	11
93	Visible luminescent lanthanide ions and a large π-conjugated ligand system shake hands. Physical Chemistry Chemical Physics, 2016, 18, 31012-31016.	1.3	11
94	Limiting Current in a Flowingâ€Electrolyteâ€Type Droplet Cell. ChemPhysChem, 2009, 10, 420-426.	1.0	10
95	Amorphous Formability and Temperature-Sensitive Luminescence of Lanthanide Coordination Glasses Linked by Thienyl, Naphthyl, and Phenyl Bridges with Ethynyl Groups. Bulletin of the Chemical Society of Japan, 2017, 90, 322-326.	2.0	10
96	Thermosensitive Seven-Coordinate TbIII Complexes with LLCT Transitions. European Journal of Inorganic Chemistry, 2018, 2018, 2031-2037.	1.0	10
97	Origin of Concentration Quenching in Ytterbium Coordination Polymers: Phonon-Assisted Energy Transfer. European Journal of Inorganic Chemistry, 2018, 2018, 561-567.	1.0	10
98	First aggregation-induced emission of a Tb(<scp>iii</scp>) luminophore based on modulation of ligand–ligand charge transfer bands. Dalton Transactions, 2020, 49, 2431-2436.	1.6	10
99	First Triboâ€Excited Chemical Reaction of a Stacked Lanthanide Coordination Polymer with an in Situ Reaction Monitor. Chemistry - A European Journal, 2021, 27, 2279-2283.	1.7	10
100	Oblique Angle Deposition of Columnar Niobium Films for Capacitor Application. Materials Transactions, 2008, 49, 1320-1326.	0.4	9
101	Mechano-electrochemistry of a passive surface using an in situ micro-indentation test. Electrochimica Acta, 2011, 56, 1773-1780.	2.6	9
102	Convection-Dependent Hydrogen Permeation into a Carbon Steel Sheet. ECS Electrochemistry Letters, 2014, 3, C21-C23.	1.9	9
103	Development of a Liquid-Phase Ion Gun and Its Application for Sulfidation of Silver Surface. Journal of the Electrochemical Society, 2015, 162, C115-C120.	1.3	9
104	Optical Characterization of Passive Oxides on Metals. Electrochemistry, 2016, 84, 826-832.	0.6	9
105	Solvent-dependent dual-luminescence properties of a europium complex with helical π-conjugated ligands. Photochemical and Photobiological Sciences, 2017, 16, 683-689.	1.6	9
106	Initiation of Localized Corrosion of Ferritic Stainless Steels by Using the Liquid-Phase Ion Gun Technique. Journal of the Electrochemical Society, 2017, 164, C1-C7.	1.3	9
107	Synthesis and Photophysical Properties of Eu(III) Complexes with Phosphine Oxide Ligands including Metal Ions. Bulletin of the Chemical Society of Japan, 2018, 91, 6-11.	2.0	9
108	Detailed Structural Analyses of Nanofibrillated Bacterial Cellulose and Its Application as Binder Material for a Display Device. Biomacromolecules, 2020, 21, 581-588.	2.6	9

#	Article	IF	CITATIONS
109	An Europiumâ€(III) Luminophore with Pressureâ€5ensing Units: Effective Back Energy Transfer in Coordination Polymers with Hexadentate Porous Stable Networks. ChemPlusChem, 2020, 85, 1989-1993.	1.3	9
110	Inhibition of field crystallization of anodic niobium oxide by incorporation of silicon species. Electrochimica Acta, 2008, 53, 8203-8210.	2.6	8
111	Acid-protected Eu(<scp>iii</scp>) coordination nanoparticles covered with polystyrene. Journal of Materials Chemistry C, 2016, 4, 75-81.	2.7	8
112	Spin-orbit coupling dependent energy transfer in luminescent nonanuclear Yb-Gd / Yb-Lu clusters. Journal of Luminescence, 2018, 201, 170-175.	1.5	8
113	First demonstration of the π–f orbital interaction depending on the coordination geometry in Eu(<scp>iii</scp>) luminophores. Dalton Transactions, 2020, 49, 3098-3101.	1.6	8
114	Current transients during repeated micro-indentation test of passive iron surface in pH 8.4 borate buffer solution. Electrochemistry Communications, 2007, 9, 1672-1676.	2.3	7
115	A numerical model for current transients during micro-indentation of passive iron surface. Electrochimica Acta, 2007, 52, 6901-6910.	2.6	7
116	Area Selective Formation of Porous Type Aluminum Anodic Oxide Film by a Solution Flow-Type Micro Droplet Cell. ECS Transactions, 2010, 33, 57-63.	0.3	7
117	SCC Mechanism Near Fusion Line of Low C-13%Cr Welded Joints. Zairyo To Kankyo/ Corrosion Engineering, 2011, 60, 196-201.	0.0	7
118	Dielectric properties of anodic films on sputter-deposited Ti–Si porous columnar films. Applied Surface Science, 2011, 257, 8295-8300.	3.1	7
119	Thermo-stable Lanthanoid Coordination Nanoparticles Composed of Luminescent Eu(III) Complexes and Organic Joint Ligands Using Micelle Techniques in Water. Bulletin of the Chemical Society of Japan, 2014, 87, 1386-1390.	2.0	7
120	Terbium Oxide, Fluoride, and Oxyfluoride Nanoparticles with Magneto-optical Properties. Bulletin of the Chemical Society of Japan, 2015, 88, 1453-1458.	2.0	7
121	Luminescent Europium(III) Coordination Zippers Linked with Thiophene-Based Bridges. Angewandte Chemie, 2016, 128, 12238-12241.	1.6	7
122	Electrochemistry for Corrosion Fundamentals. Springer Briefs in Molecular Science, 2018, , .	0.1	7
123	On the Electropolishing Mechanism of Nickel Titanium in Methanolic Sulfuric acid â^' An Electrochemical Impedance Study. Physica Status Solidi (A) Applications and Materials Science, 2018, 215, 1800011.	0.8	7
124	Preparation of boron-containing carbons from glucose–borate complexes and their capacitive performance. Tanso, 2009, 2009, 156-161.	0.1	7
125	Preparation of photonic molecular trains via soft-crystal polymerization of lanthanide complexes. Nature Communications, 2022, 13, .	5.8	7
126	Controlled morphology of aluminum alloy nanopillar films: from nanohorns to nanoplates. Nanotechnology, 2010, 21, 395302.	1.3	6

#	Article	IF	CITATIONS
127	Titanium surface anodized under UV light irradiation observed by ellipso-microscopy. Journal of Solid State Electrochemistry, 2015, 19, 3579-3587.	1.2	6
128	J-Type Heteroexciton Coupling Effect on an Asymmetric Donor–Acceptor–Donor-Type Fluorophore. Journal of Physical Chemistry A, 2017, 121, 4613-4618.	1.1	6
129	Micro- and Nano-Scopic Aspects of Passive Surface on Pearlite Structure of Carbon Steel in pH 8.4 Boric Acid-Borate Buffer. Journal of the Electrochemical Society, 2019, 166, C3409-C3416.	1.3	6
130	Bright sky-blue fluorescence with high color purity: assembly of luminescent diphenyl-anthracene lutetium-based coordination polymer. RSC Advances, 2021, 11, 6604-6606.	1.7	6
131	Development of a Low Solution Resistance Type Solution Flow Droplet Cell and Investigation of Its Electrochemical Performance. ISIJ International, 2010, 50, 1466-1470.	0.6	6
132	EuS Nano-assembles Linked with Photo-functional Naphthalenedithiols. Molecular Crystals and Liquid Crystals, 2013, 579, 69-76.	0.4	5
133	Formation of Area and Thickness Controlled Porous Type Aluminum Anodic Oxide Films by Sf-MDC. ECS Transactions, 2013, 50, 255-262.	0.3	5
134	Chiroptical Properties of Nonanuclear Tb(III) Clusters with Chiral Champhor Derivative Ligands. E-Journal of Surface Science and Nanotechnology, 2015, 13, 31-34.	0.1	5
135	Circularly Polarized Absorption and Luminescence of Semiconductor Euâ€OCN Nanocrystals in the Blue Region of the Electromagnetic Spectrum. ChemPhysChem, 2020, 21, 2019-2024.	1.0	5
136	Long-lived emission beyond 1000 nm: control of excited-state dynamics in a dinuclear Tb(<scp>iii</scp>)–Nd(<scp>iii</scp>) complex. Chemical Communications, 2021, 57, 8047-8050.	2.2	5
137	Thermoâ€Sensitive Eu ^{III} Coordination Polymers with Amorphous Networks. ChemistrySelect, 2021, 6, 2812-2816.	0.7	5
138	Asymmetric Lumino-Transformer: Circularly Polarized Luminescence of Chiral Eu(III) Coordination Polymer with Phase-Transition Behavior. Journal of Physical Chemistry B, 2022, 126, 3799-3807.	1.2	5
139	Evaluation of Materials Surface Using Capillary Micro-cell Technique. Hyomen Gijutsu/Journal of the Surface Finishing Society of Japan, 2008, 59, 863-863.	0.1	4
140	Growth of Porous Anodic Films on Niobium in Hot Phosphate-Glycerol Electrolyte. ECS Transactions, 2008, 16, 345-351.	0.3	4
141	Local Cu Electro-Plating on Non-Conductive Substrate and Fabrication of Metal Structure with Solution Flow Type Micro-Droplet Cell. Hyomen Gijutsu/Journal of the Surface Finishing Society of Japan, 2011, 62, 511-515.	0.1	4
142	Heterogeneity of a Thermal Oxide Film Formed on Polycrystalline Iron Observed by Two-Dimensional Ellipsometry. Journal of the Electrochemical Society, 2016, 163, C815-C822.	1.3	4
143	Highly luminescent tetranuclear Eu(III) complex with characteristic cavity space. Inorganica Chimica Acta, 2019, 486, 240-244.	1.2	4
144	Active-Passive Transition of an Fe-6 mass% Cr Surface in Acidic Sodium Sulfate Solutions Under a Laminar Flow Condition Evaluated by Ellipso-Microscopy and Channel Flow Electrode Method. Journal of the Electrochemical Society, 2021, 168, 051503.	1.3	4

#	Article	IF	CITATIONS
145	Electrochemical Noise Analysis of 13 mass% Cr Stainless Steel HAZ by Solution Flow Type Micro-droplet Cell-Effect of Solution Concentration ECS Transactions, 2009, 16, 281-290.	0.3	3
146	Investigation of Depassivation-repassivation Behavior of Metal Surfaces Using Micro-indentation Test. Zairyo To Kankyo/ Corrosion Engineering, 2011, 60, 28-38.	0.0	3
147	Microelectrochemistry at Heat-tinted Zone of Stainless Steel Weldment. Zairyo To Kankyo/ Corrosion Engineering, 2015, 64, 552-557.	0.0	3
148	Thermostable Nano Luminophores Composed of Europium Ions and Organic Ligands. E-Journal of Surface Science and Nanotechnology, 2015, 13, 219-222.	0.1	3
149	An Estimation Method of Metalâ€Ligand Orbital Mixing in Lanthanide(III) Complexes Using Magnetic Circular Dichroism. ChemistrySelect, 2018, 3, 2646-2648.	0.7	3
150	Aggregation-induced emission of a Eu(III) complex via ligand-to-metal charge transfer. Chemical Physics Letters, 2020, 749, 137437.	1.2	3
151	Photolithographic Fabrication of a Micro-electrode Surface on a Carbon Steel Sheet for Local Hydrogen Permeation Measurements. ISIJ International, 2021, 61, 1112-1119.	0.6	3
152	Amide-bridged Eu(III) coordination polymer for stable luminescent glass material. Materials Letters, 2021, 297, 130012.	1.3	3
153	Hybrid Eu III Coordination Luminophore Standing on Two Legs on Silica Nanoparticles for Enhanced Luminescence. Chemistry - A European Journal, 2021, 27, 14438-14443.	1.7	3
154	Scanning Electrochemical Microscopic Study of Detecting Non-homogeneity in Surface Reactions of Metals ISIJ International, 2002, 42, 1326-1333.	0.6	3
155	FEM Analysis for Sinusoidal Perturbation of Hydrogen Permeation into a Steel Sheet. ISIJ International, 2016, 56, 472-477.	0.6	3
156	Effective Photosensitization in Excited‣tate Equilibrium: Brilliant Luminescence of Tb ^{III} Coordination Polymers Through Ancillary Ligand Modifications. ChemPlusChem, 2022, 87, .	1.3	3
157	Electroluminescence from p-type silicon during anodic oxidation in ethylene glycol solution. Journal of Electroanalytical Chemistry, 1994, 368, 257-264.	1.9	2
158	Performance of a microelectrode vibrating above an insulator surface. Electrochemistry Communications, 2004, 6, 959-963.	2.3	2
159	Electrochemical Capacitance of Nitrogen-Containing Nanocarbons Prepared Using Porous Anodic Alumina Template. Electrochemistry, 2008, 76, 197-202.	0.6	2
160	The Effect of Metal Texture on Depassivation-repassivation Behavior of Iron in Borate Buffer Solution Investigated by Micro-indentation. ECS Transactions, 2009, 16, 133-140.	0.3	2
161	Anodic Behavior of Nickel in Acidic Perchlorate Solution Containing Pb ²⁺ . ECS Transactions, 2009, 16, 109-116.	0.3	2
162	Depassivation pH of Austenitic Stainless Steels in NaCl Aqueous Solution. ECS Transactions, 2009, 16, 291-296.	0.3	2

#	Article	IF	CITATIONS
163	Shielding effect of double microelectrode tips in a scanning electrochemical microscope. Electrochimica Acta, 2011, 56, 9602-9608.	2.6	2
164	Simple heat treatment for fabrication of carbonaceous layer-coated microelectrodes and conductive stainless steels. Applied Surface Science, 2011, 257, 8289-8294.	3.1	2
165	Effects of thickness and field strength of anodic oxide film on aluminum on its compressive rupture. Corrosion Reviews, 2012, 30, .	1.0	2
166	Luminescent Silicon Nanoparticles Surface-Modified with Chiral Molecules. Journal of Photopolymer Science and Technology = [Fotoporima Konwakai Shi], 2015, 28, 255-260.	0.1	2
167	Synthesis and Photoluminescence Properties of Nonanuclear Tb(III) Clusters with Long Alkyl Chain Group. E-Journal of Surface Science and Nanotechnology, 2015, 13, 27-30.	0.1	2
168	Photoswitchable Faraday effect in EuS–Au nanosystems. Physica Status Solidi (A) Applications and Materials Science, 2016, 213, 178-182.	0.8	2
169	Liquid-Phase Ion Gun Technique for Degradation and Evaluation of Oxide Films. ECS Transactions, 2017, 75, 3-8.	0.3	2
170	Some microelectrochemical methods for the investigation of passivity and corrosion. Corrosion Reviews, 2018, 36, 3-15.	1.0	2
171	Time-Dependent Measurement of Hydrogen Penetration into Iron Sheets from a Borate Buffer Solution Using FFT Analysis. Journal of the Electrochemical Society, 2018, 165, C900-C906.	1.3	2
172	Liquid-Phase Ion Gun for Local Acidification of Na2S Aqueous Solution and Local Sulfidation of Fe-Cr Alloy Surface. Journal of the Electrochemical Society, 2018, 165, C618-C623.	1.3	2
173	Effect of intentional convection on the passivity of an Fe–6Cr surface in pH 4.5 Na2SO4 solution. Electrochimica Acta, 2020, 346, 136237.	2.6	2
174	Triboâ€Excited Chemical Reaction Using an Eu ^{III} Complex with a Stacked Anthracene Framework. Chemistry - A European Journal, 2022, 28, e202200593.	1.7	2
175	Fabrication of Micro-disk Electrode Probe by Electroless Nickel Plating. Hyomen Gijutsu/Journal of the Surface Finishing Society of Japan, 2006, 57, 592-596.	0.1	1
176	Current Transients from Passive Iron Surface during Micro-indentation. ECS Transactions, 2006, 1, 367-378.	0.3	1
177	Effect of Cold Rolling on Passive Film on Pure Iron in pH 8.4 Borate Buffer Solution. ECS Transactions, 2010, 25, 3-15.	0.3	1
178	Anodic Dissolution of Titanium in Ethylene Glycol Solution Containing Chloride Salt. ECS Transactions, 2010, 25, 111-117.	0.3	1
179	GDOES Depth Profile Analysis of Interfacial Enrichment of Copper during Anodizing of Al-Cu Alloy. Hyomen Cijutsu/Journal of the Surface Finishing Society of Japan, 2015, 66, 670-672.	0.1	1
180	Synthesis of TbO <i>_x</i> Nanoparticles from the Thermal Decomposition of Tb(III) Complexes. E-Journal of Surface Science and Nanotechnology, 2015, 13, 23-26.	0.1	1

Којі Ғизнімі

#	Article	IF	CITATIONS
181	Hydrogen Embrittlement and Hydrogen Absorption. Springer Briefs in Molecular Science, 2018, , 79-96.	0.1	1
182	Asymmetric Colorâ€Changeable Luminophore with Donor–Acceptor–Donor Structure for Solvent and Temperature Sensitive Properties. ChemistrySelect, 2018, 3, 10905-10908.	0.7	1
183	Combinatorial Passivation Study in the Aluminium-Samarium System for Basic Property Mapping and Identification of Secondary Phase Influence. Journal of the Electrochemical Society, 2021, 168, 011503.	1.3	1
184	Rapid Method to Measure Hydrogen Diffusion Coefficient in Metal Using a Multi-sine Wave Signal. ISIJ International, 2021, 61, 1064-1070.	0.6	1
185	Micro-electrochemical Approach for Corrosion Study. Springer Briefs in Molecular Science, 2018, , 97-116.	0.1	1
186	Formation of Porous Aluminum Films with Isolated Columnar Structure Using Physical Vapor Deposition for Medium-Voltage and High-voltage Capacitors. Hyomen Gijutsu/Journal of the Surface Finishing Society of Japan, 2009, 60, 166-169.	0.1	1
187	Ellipso-Microscopic Observation of Titanium Surface under UV-Light Irradiation. Corrosion Science and Technology, 2016, 15, 265-270.	0.2	1
188	Hydrogen Permeation into a Carbon Steel Sheet Observed by a Micro-capillary Combined with a Devanathan-Stachurski Cell. Tetsu-To-Hagane/Journal of the Iron and Steel Institute of Japan, 2019, 105, 64-68.	0.1	1
189	Triboâ€excited Chemical Reaction Using EuIII Complex with Stacked Anthracene Frameworks. Chemistry - A European Journal, 2022, , .	1.7	1
190	Evaluation and Analytical Method for Hydrogen Embrittlement. Zairyo/Journal of the Society of Materials Science, Japan, 2022, 71, 548-552.	0.1	1
191	Lithium ion insertion/extraction performance of Si/C/O composites formed from polyimides containing silicone. Tanso, 2009, 2009, 207-212.	0.1	Ο
192	Origin of Concentration Quenching in Ytterbium Coordination Polymers: Phononâ€Assisted Energy Transfer. European Journal of Inorganic Chemistry, 2018, 2018, 545-545.	1.0	0
193	Identification of Passive Films and Corrosion Products. Springer Briefs in Molecular Science, 2018, , 41-63.	0.1	Ο
194	III. Advanced Electrochemical Methods for Corrosion Studyï¼5canning Electrochemical Microscopy ï¼^SECM)5 Zairyo To Kankyo/ Corrosion Engineering, 2018, 67, 109-114.	0.0	0
195	Current Transients of Passive Iron during Micro-indentation in Solution. , 2006, , 451-456.		Ο
196	Electrochemical Fundamentals of Corrosion and Corrosion Protection. Springer Briefs in Molecular Science, 2018, , 1-15.	0.1	0
197	Electrochemical Measurement of Atmospheric Corrosion. Springer Briefs in Molecular Science, 2018, , 65-78.	0.1	Ο
198	<i>In-situ</i> Imaging of Anodizing Titanium Oxide Film. Hyomen Gijutsu/Journal of the Surface Finishing Society of Japan, 2018, 69, 22-27.	0.1	0

#	Article	IF	CITATIONS
199	A Liquid-phase Ion Gun Technique for Generating Sulfide Ions on Metal Surfaces. Zairyo To Kankyo/ Corrosion Engineering, 2019, 68, 120-127.	0.0	0
200	<i>In-situ</i> Observation of Corrosion Initiation Occurring on NaCl Nanoparticles-deposited Carbon Steel Surfaces. Tetsu-To-Hagane/Journal of the Iron and Steel Institute of Japan, 2021, 107, 1011-1019.	0.1	0